

Thiophene Hydrodesulfurization over Alumina-Supported Molybdenum Carbide and Nitride Catalysts: Adsorption Sites, Catalytic Activities, and Nature of the Active Surface

Paul A. Aegerter, Wes W. C. Quigley, Garth J. Simpson, David D. Ziegler, John W. Logan, Keith R. McCrea, Samantha Glazier, and Mark E. Bussell¹

Department of Chemistry, M.S.-9150, Western Washington University, Bellingham, Washington 98225

Received April 4, 1996; revised July 29, 1996; accepted July 30, 1996

Mo₂C/Al₂O₃ and Mo₂N/Al₂O₃ catalysts have been synthesized and characterized by X-ray diffraction, pulsed chemisorption (CO and O₂) and infrared (IR) spectroscopy, and temperature programmed desorption (TPD) measurements. Thiophene hydrodesulfurization (HDS) activities were measured for alumina-supported Mo carbide and nitride catalysts as well as a sulfided Mo/Al₂O₃ catalyst, all with a 10 wt% Mo loading. The HDS activities ($\mu\text{mol Th/mol Mo/s}$) of the catalysts after 24 h at 693 K were found to increase according to the trend sulfided Mo < γ -Mo₂N < β -Mo₂C, and provide further evidence that carbide and nitride catalysts have the potential to replace sulfided Mo catalysts in commercial HDS reactors. X-ray diffraction analysis of fresh and tested 30 wt% Mo₂C/Al₂O₃ and Mo₂N/Al₂O₃ catalysts indicates that the bulk structure of the carbide (β -Mo₂C) and nitride (γ -Mo₂N) particles is retained, while IR spectroscopy of adsorbed CO indicates that the surface of the carbide and nitride particles becomes sulfided under reaction conditions. A model is proposed for the structure of the active catalytic surface of the alumina-supported Mo carbide and nitride catalysts in which a thin layer of highly dispersed sulfided Mo is present on the surfaces of the carbide and nitride particles.

© 1996 Academic Press, Inc.

INTRODUCTION

More stringent environmental legislation and the need to utilize low quality hydrocarbon feedstocks have focused increased attention on the catalytic processes involved in converting these feeds into clean burning fuels. Chianelli *et al.* have recently discussed the need to develop a new generation of catalysts for the removal of sulfur and nitrogen impurities from low quality feedstocks (1). Because they exhibit catalytic properties similar to group VIII metals (2), early transition metal carbides and nitrides have attracted attention for a number of catalytic reactions and have demonstrated strong potential for use in both the hydrodenitrogenation (HDN) (3–10) and hydrodesulfurization (HDS) (4, 5, 8, 11–13) processes.

Focussing on hydrodesulfurization, Lee and Boudart found unsupported α -MoC_(1-x) ($x \approx 0.5$) to have a thiophene HDS activity similar to that of a sulfided Mo/Al₂O₃ catalyst (11), while Sajkowski and Oyama found an alumina-supported β -Mo₂C catalyst (Mo₂C/Al₂O₃) to have an HDS activity over two times greater than that of a commercial Ni-Mo/Al₂O₃ catalyst (Shell 324) for a coal-derived liquid feed (4, 5). Molybdenum nitride has also shown promise for use in the HDS process. In the study mentioned above, Sajkowski and Oyama found unsupported Mo₂N to be nearly twice as active as the commercial Ni-Mo/Al₂O₃ catalyst for HDS of the same coal-derived feed (4, 5). Both Abe *et al.* (9) and Markel *et al.* (12) found unsupported Mo₂N to be active for HDS of benzothiophene and thiophene, respectively, and the latter study also showed that the bulk structure of the molybdenum nitride was preserved despite the sulfiding conditions present in the catalytic reactor. Finally, Nagai and co-workers investigated dibenzothiophene HDS over alumina-supported Mo₂N and found the nitride to be 1.1–1.2 times more active than a sulfided Mo/Al₂O₃ catalyst under identical reaction conditions (13).

One of the difficulties encountered when comparing the catalytic activities of carbide and nitride catalysts with those of sulfide catalysts is choosing an appropriate measure of active sites for the different catalysts. The number of active sites on carbide and nitride catalysts has typically been estimated by CO chemisorption (2, 14), while oxygen chemisorption is normally employed for sulfides (15). The HDS activity of sulfided Mo/Al₂O₃ catalysts has been shown to correlate with both their CO and O₂ chemisorption capacities (15–17). These probe molecules selectively adsorb on coordinately unsaturated Mo²⁺ sites located on the edge planes of MoS₂ crystallites which are thought to be the active sites for hydrodesulfurization (18–20). For carbide and nitride catalysts, little is known about the sites on which CO and O₂ adsorb and what the relationship is between these adsorption sites and the active sites for hydrodesulfurization.

¹ To whom correspondence should be addressed.

The purpose of the current study is twofold: (1) to establish a meaningful comparison of the thiophene HDS activity of $\text{Mo}_2\text{C}/\text{Al}_2\text{O}_3$, $\text{Mo}_2\text{N}/\text{Al}_2\text{O}_3$ and sulfided $\text{Mo}/\text{Al}_2\text{O}_3$ catalysts and (2) to investigate the relationship between the CO chemisorption sites of the fresh catalysts and those of catalysts subjected to sulfiding conditions similar to those present in a thiophene HDS flow reactor using (IR) spectroscopy and temperature programmed desorption (TPD).

EXPERIMENTAL SECTION

Catalyst Preparation

Alumina-supported molybdenum trioxide ($\text{MoO}_3/\text{Al}_2\text{O}_3$) catalysts were prepared by impregnation of $\gamma\text{-Al}_2\text{O}_3$ (Engelhard AL-3945) with aqueous solutions of ammonium heptamolybdate (J. T. Baker Co.). Catalysts with Mo loadings of 10, 20, and 30 wt% were prepared. The latter two catalysts required multiple impregnations to achieve the desired Mo loading. The $\gamma\text{-Al}_2\text{O}_3$ had a BET surface area of $255\text{ m}^2/\text{g}$ and a pore volume of 0.60 ml/g . The alumina support (1/12 in. extrusions) was ground to a fine powder prior to use. Following impregnation, the catalysts were dried for 24 h at 393 K and then calcined for 3 h in air at 773 K. Bulk and alumina-supported molybdenum carbide and nitride catalysts were prepared according to the procedures outlined by Lee *et al.* (14, 21). Catalyst synthesis was accomplished via temperature programmed reduction (TPR) in an atmospheric pressure flow system outfitted with a quartz U-tube type reactor, a stainless steel gas manifold, mass flow controllers (MKS Instruments), and a furnace composed of a ceramic fiber heater (Watlow) and a temperature controller (Watlow). A typical synthesis employed 0.1–1.0 g of $\text{MoO}_3/\text{Al}_2\text{O}_3$ supported on a plug of quartz wool; the oxide precursor was outgassed for 1 h at 673 K in a 30 sccm/min flow of He (Airco, 99.999%) prior to switching to a flow of the reducing gas. The He was purified prior to use by passing through 5A molecular sieve (Alltech) and O_2 (Oxyclear) purification traps. The preparation of bulk and alumina-supported Mo_2N catalysts involved heating the oxide precursor in a 60 sccm/min flow of anhydrous ammonia (Airco, 99.99%) using TPR from 673 K to 950 K at a heating rate of 30 K/h. The synthesis procedure for bulk and alumina-supported Mo_2C catalysts utilized the same TPR program with a 60 sccm/min flow of a 20 mol% CH_4/H_2 mixture (Airco, CH_4 99%, H_2 99.97%). The CH_4/H_2 mixture was purified prior to use by passing it through a trap system similar to the one described above for He. Following synthesis, $\text{Mo}_2\text{C}/\text{Al}_2\text{O}_3$ and $\text{Mo}_2\text{N}/\text{Al}_2\text{O}_3$ catalysts were cooled to room temperature in flowing He (30 sccm/min) and then passivated in a 30 sccm/min flow of a 1% O_2/He mixture (Airco) at 298 K for 3 h prior to their removal from the flow system. Sulfided $\text{Mo}/\text{Al}_2\text{O}_3$ catalysts were synthesized *in situ* for pulsed chemisorption, catalytic reactor, and IR-TPD studies. Following outgassing in

flowing He at 673 K, oxidic precursors were sulfided in a 60 sccm/min flow of a 3.03% $\text{H}_2\text{S}/\text{H}_2$ mixture (Airco) at 623 K for 2 h for pulsed chemisorption and catalytic reactor studies. Sulfided catalysts subjected to IR-TPD studies in an ultrahigh vacuum (UHV) chamber were synthesized from oxidic precursors via two consecutive sulfidation treatments consisting of heating to 623 K in 100 Torr (1 Torr = 133.3 N/m^2) of a 3.03% $\text{H}_2\text{S}/\text{H}_2$ mixture for 30 min. The catalyst samples were outgassed prior to sulfidation and after each treatment by heating to 623 K in UHV for 30 min.

X-Ray Diffraction Measurements

Crystalline phases of bulk and alumina-supported molybdenum carbide and nitride catalysts were determined by X-ray diffraction using the packed powder method. Both freshly synthesized and tested catalysts were passivated in a 1% O_2/He flow (298 K, 3 h) prior to transfer to the X-ray diffractometer. Diffraction patterns were acquired using a Rigaku Geigerflex Diffractometer and $\text{CuK}\alpha$ radiation ($\lambda = 1.5418\text{ \AA}$) and are reproduced here without any background or smoothing treatment.

BET and Pulsed Chemisorption Measurements

BET surface area and pulsed chemisorption (CO and O_2) measurements were carried out using a Micromeritics Pulse Chemisorb 2700 apparatus. For both types of measurements, catalyst samples ($\sim 0.10\text{ g}$) were placed in a quartz U-tube (15 mm OD), where they were degassed in flowing He (45 sccm/min) at 673 K for 2 h. $\text{Mo}_2\text{C}/\text{Al}_2\text{O}_3$ and $\text{Mo}_2\text{N}/\text{Al}_2\text{O}_3$ catalysts were then activated by heating to 750 K for 2 h in a 60 sccm/min flow of H_2 . Sulfided $\text{Mo}/\text{Al}_2\text{O}_3$ catalysts were prepared as described above and subsequently reduced at 623 K in a 60 sccm/min flow of H_2 for 1 h. Additional chemisorption experiments were carried out to determine the effects of sulfidation on the CO and O_2 chemisorption capacities of the carbide and nitride catalysts. Following activation, $\text{Mo}_2\text{C}/\text{Al}_2\text{O}_3$ and $\text{Mo}_2\text{N}/\text{Al}_2\text{O}_3$ catalysts were sulfided *in situ* (60 sccm/min flow of a 3.03% $\text{H}_2\text{S}/\text{H}_2$ mixture at 623 K for 2 h) followed by reduction in flowing H_2 at 623 K for 1 h. Prior to the BET and chemisorption measurements, the carbide, nitride, and sulfide catalysts were subjected to a final outgassing treatment in which they were heated to 673 K in flowing He (45 sccm/min) for 1 h. The He and H_2 used in the chemisorption system were passed through 5A molecular sieve and O_2 purification traps prior to use.

Single point BET surface area measurements were carried out using a 28.6% N_2/He mixture (Airco). The instrument was calibrated prior to the BET measurements using pure N_2 gas.

Chemisorption capacities were measured by injecting a calibrated sample loop of gas, CO (Airco, 99.99%) or O_2

(Airco, 10.3% in He), into an He flow (45 sccm/min for CO, 15 sccm/min for O₂) passing over the catalysts at 1 min intervals until gas uptake ceased. Prior to injection, the CO was passed through a coil of 1/8" stainless steel tubing submerged in a pentane slush to remove metal carbonyl impurities. O₂ and CO chemisorption studies were performed at 196 and 273 K, respectively. Fresh catalyst samples were prepared for each chemisorption measurement.

Thiophene HDS Activity Measurements

Thiophene HDS activity measurements were carried out using an atmospheric pressure flow reactor outfitted with a gas chromatograph (HP 5890 Series II) equipped with a flame ionization detector for on-line analysis of thiophene and hydrocarbon products. The gas chromatograph is interfaced to a personal computer on which HP Chemstation software has been installed for automated sampling procedures. Gas flows were maintained using mass-flow controllers (MKS Instruments). Catalyst samples (~0.10 g) were supported on a quartz wool plug in a quartz U-tube reactor (15 mm OD) in a 50 sccm/min flow of a 1.8% thiophene/H₂ mixture prepared by means of a two-stage thiophene bubbler apparatus. The thiophene used in this study (Aldrich Chemical Co., 99+% purity) was purified according to the procedure of Spies and Angelici prior to use in order to remove thiol impurities (22). The reaction temperature was maintained using a ceramic-fiber furnace (Watlow) outfitted with a programmable temperature controller (Omega). Mo₂C/Al₂O₃ and Mo₂N/Al₂O₃ catalysts were degassed in a 30 sccm/min flow of He at 673 K for 1 h, activated in a 60 sccm/min flow of H₂ at 750 K, and then cooled to the desired reaction temperature prior to switching to the thiophene/H₂ flow. Sulfided Mo/Al₂O₃ catalysts were prepared as described above, outgassed in flowing He (30 sccm/min) at the desired reaction temperature for 30 min, and the flow then switched to the thiophene/H₂ mixture. Thiophene HDS conversion data were collected at 1 h intervals over 24 h at a reaction temperature of 693 K. Steady state conversion was achieved after ~16 h; catalyst activities reported here are the values after 24 h on stream. The major HDS products (butadiene, 1-butene, *cis*-2-butene, *trans*-2 butene, and butane) and unreacted thiophene were separated using a 30 m GS-Alumina column (J & W Scientific). C₁-C₃ hydrocarbons totalled <1% of the products and were neglected in selectivity calculations. The detector response for the C₄ hydrocarbon products was calibrated with analytical gas standards (Scott) to facilitate conversion calculations.

Infrared Spectroscopy Measurements

Experiments were carried out in a bakeable, stainless-steel ultrahigh-vacuum system pumped by a 110 liter/s ion pump and equipped with a high pressure cell that could be

isolated from the vacuum chamber; the system has been described in detail elsewhere (23). Catalyst samples (~10 mg, 1 cm²) were pressed into a nickel metal mesh (50 × 50 mesh size, 0.002 in. wire diameter) and mounted on the sample holder. For the purpose of temperature measurement, a chromel-alumel thermocouple is spot-welded to the top edge of the Ni mesh. Following introduction into the UHV system, catalyst samples were outgassed at 475 K for 16 h. Typical system base pressure following such a procedure was ~5.0 × 10⁻⁹ Torr. Mo₂C/Al₂O₃ and Mo₂N/Al₂O₃ catalysts were activated in a 60 sccm/min atmospheric pressure flow of H₂ at 750 K for 2 h followed by outgassing in UHV at 673 K. To prepare sulfided Mo/Al₂O₃ catalysts, oxidic catalyst samples were outgassed and sulfided *in situ* as described above. Following sulfidation, the catalysts were reduced in 60 sccm/min flow of H₂ at 623 K for 1 h.

IR spectral acquisition was accomplished using Mattson RS-1 FTIR spectrometer equipped with a narrow band MCT detector and consisted of 1024 scans of the region 4000-1000 cm⁻¹, which took approximately 5 min to acquire. Depending upon the experiment, background spectra were acquired for a blank nickel mesh in either UHV or 5.0 Torr CO at 298 K. Two kinds of experiments were carried out. The first set of experiments examined the adsorption of CO on passivated and freshly activated 20% Mo₂C/Al₂O₃ catalysts. Following outgassing in UHV, a catalyst sample was cooled to 130 K and exposed to 5.0 Torr of CO. The high pressure cell was then evacuated, and the catalyst sample exposed to UHV. Following acquisition of an IR spectrum at 130 K, a TPD experiment was carried out over the temperature range 130-700 K while acquiring mass spectral data for *m/e* = 28. The sample was then warmed to room temperature and activated in flowing H₂ as described above. Following outgassing, the sample was again cooled to 130 K, exposed to 5.0 Torr of CO, and IR and TPD spectra acquired in UHV. The sample spectra acquired in these experiments were ratioed with a background spectrum acquired for a blank Ni mesh in UHV.

The second set of IR experiments was carried out for catalysts with a 10 wt% Mo loading and consisted of the following sequence. IR spectra were acquired for a freshly prepared sample in UHV and after exposure to an equilibrium pressure of 5.0 Torr CO, both at 298 K. Following the second IR spectral acquisition, the samples were evacuated to UHV and flashed to 600 K to remove residual adsorbed CO. Catalysts were then treated in an atmosphere of 5.0 Torr thiophene and 750 Torr H₂ at 400 K for 1 h. Upon completion of the thiophene/H₂ treatment, the high pressure cell was evacuated to UHV and the sample outgassed by heating at a rate of 1 K/s to 750 K and holding at this temperature for 2 min. Following sample cooling to 298 K, the IR spectral acquisition procedure described above was repeated. This experimental sequence was repeated for thiophene/H₂ treatments at 100 K increments from 400-700 K. The sample

IR spectra from these experiments were ratioed with the spectrum of a blank Ni mesh in 5.0 Torr of CO.

For TPD experiments, the UHV system is outfitted with a Leybold-Inficon Quadrex 200 quadrupole mass spectrometer which is also interfaced to a personal computer. TPD experiments were carried out using a heating rate of 1 K/s while acquiring data ($m/e = 28$) at a sampling frequency of 2 points/K. The TPD spectra are reproduced here without any background or smoothing treatment.

RESULTS

X-Ray Diffraction Analysis of Passivated $\text{Mo}_2\text{C}/\text{Al}_2\text{O}_3$ and $\text{Mo}_2\text{N}/\text{Al}_2\text{O}_3$ Catalysts

X-ray diffraction analysis of bulk and alumina-supported molybdenum carbide and nitride catalysts permitted identification of crystalline Mo phases for loadings at which three dimensional particles are present on the alumina support. For an Mo loading of 30 wt%, X-ray diffraction patterns for $\text{Mo}_2\text{C}/\text{Al}_2\text{O}_3$ and $\text{Mo}_2\text{N}/\text{Al}_2\text{O}_3$ catalysts exhibit a number of the diffraction peaks observed for bulk $\beta\text{-Mo}_2\text{C}$ and $\gamma\text{-Mo}_2\text{N}$, respectively (see Figs. 5 and 6). The diffraction pattern for a 30 wt% $\text{Mo}_2\text{C}/\text{Al}_2\text{O}_3$ catalyst shows peaks at 34.7° , 38.0° , 39.8° , 62.1° , and 75.5° plus additional peaks which can be assigned to the $\gamma\text{-Al}_2\text{O}_3$ support. The first four peaks are assigned to the {100}, {002}, {101}, and {110} reflections of bulk $\beta\text{-Mo}_2\text{C}$, respectively, while the last peak is composed of an unresolved doublet assigned to the {112} and {201} reflections of this same material (24). Using the Scherrer equation and the width at half height of the {101} reflection, a $\beta\text{-Mo}_2\text{C}$ particle size of ~ 60 Å can be estimated for the 30 wt% $\text{Mo}_2\text{C}/\text{Al}_2\text{O}_3$ catalyst. The diffraction pattern for a 30 wt% $\text{Mo}_2\text{N}/\text{Al}_2\text{O}_3$ catalyst shows peaks at 38.2° , 44.2° , 64.0° , and 76.7° which are assigned to the {111}, {200}, {220}, and {311} reflections of bulk $\gamma\text{-Mo}_2\text{N}$, respectively (25). A $\gamma\text{-Mo}_2\text{N}$ particle size of ~ 60 Å can be estimated using the width at half height of the {200} reflection for the 30 wt% $\text{Mo}_2\text{N}/\text{Al}_2\text{O}_3$ catalyst. The alpha phase of molybdenum carbide ($\alpha\text{-MoC}_{(1-x)}$ ($x = 0.5$)) can also be prepared on $\gamma\text{-Al}_2\text{O}_3$ (14, 21, 26), but its HDS properties were not investigated in this study.

TABLE 1

BET Surface Areas and Chemisorption Data for Fresh Catalysts (10 wt% Mo)

Catalyst	Surface area (m^2/g)	CO uptake (273 K) ($\mu\text{mol CO}/\text{g}$)	O_2 uptake (196 K) ($\mu\text{mol O}_2/\text{g}$)
Sulfided $\text{Mo}/\text{Al}_2\text{O}_3$	215	37	50
$\text{Mo}_2\text{N}/\text{Al}_2\text{O}_3$	196	78	115
$\text{Mo}_2\text{C}/\text{Al}_2\text{O}_3$	205	69	111

BET Surface Areas and Chemisorption Capacities of Activated $\text{Mo}_2\text{C}/\text{Al}_2\text{O}_3$ and $\text{Mo}_2\text{N}/\text{Al}_2\text{O}_3$ Catalysts

The BET surface area as well as the CO and O_2 chemisorption capacities of alumina-supported Mo carbide, nitride, and sulfided Mo catalysts with 10 wt% Mo loading are summarized in Table 1. The alumina support used in this study adsorbed neither CO nor O_2 at the temperatures (273 and 196 K, respectively) at which the chemisorption measurements were conducted.

IR Spectroscopy of CO on Passivated and Activated 20 wt% $\text{Mo}_2\text{C}/\text{Al}_2\text{O}_3$ Catalysts

A sample of a passivated 20 wt% $\text{Mo}_2\text{C}/\text{Al}_2\text{O}_3$ catalyst was mounted in the UHV system and outgassed as described in the Experimental Section. Following cooling to 130 K and exposure to an equilibrium pressure of 5.0 Torr for approximately 5 min, the sample was evacuated to UHV pressures and an IR spectrum acquired in the ν_{CO} region (Fig. 1). Subsequent to the IR spectral acquisition, a temperature programmed desorption spectrum was acquired over the range 130–700 K, as will be discussed below. The IR spectrum of CO on the passivated 20 wt% $\text{Mo}_2\text{C}/\text{Al}_2\text{O}_3$ catalyst displays a single ν_{CO} band at 2199 cm^{-1} , which is assigned to weakly chemisorbed CO bonded to coordinately unsaturated (*cus*) Al^{3+} sites of the $\gamma\text{-Al}_2\text{O}_3$ support. This assignment is consistent with previous studies of

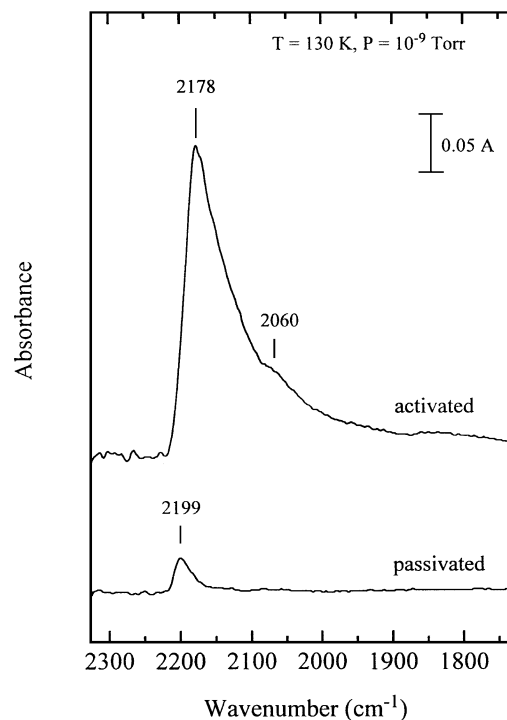


FIG. 1. IR spectra for a passivated and activated 20% $\text{Mo}_2\text{C}/\text{Al}_2\text{O}_3$ catalyst dosed with 5.0 Torr of CO at 130 K and then evacuated to UHV.

CO adsorption on pure γ -Al₂O₃ conducted in this (23) and other laboratories (27). Based upon these IR results, it can be concluded that passivation of a 20 wt% Mo₂C/Al₂O₃ catalyst renders the Mo₂C particles inert to the adsorption of CO at 130 K.

Following the CO adsorption studies on a sample of passivated Mo₂C/Al₂O₃, the catalyst sample was activated by heating in flowing H₂ as described earlier. The catalyst was then outgassed in UHV at 673 K, cooled to 130 K, and exposed to an equilibrium pressure of 5.0 Torr of CO for approximately 5 min. Following evacuation in UHV, IR (Fig. 1) and TPD spectra were acquired. Activation in flowing H₂ produces substantial changes in the CO adsorption properties of the carbide catalyst as revealed by the IR spectrum. Two ν_{CO} features are apparent in the IR spectrum for the activated catalyst at 2178 and 2060 cm⁻¹. To our knowledge, this is the first IR spectrum for adsorbed CO on a Mo₂C/Al₂O₃ catalyst to appear in the literature, but information to aid in the assignment of the observed IR bands is available from a number of related studies. Using high resolution electron energy loss spectroscopy (HREELS), Fr berger and Chen observed three adsorbed CO species on a Mo(110) single crystal with a surface carbide layer (28). ν_{CO} bands at 1850 and 2015 cm⁻¹ were assigned to bridge and terminally bonded CO species, respectively, while a very weak band at 1150 cm⁻¹ was assigned to a "side-on" CO species. Wang *et al.* used reflectance absorbance infrared spectroscopy (RAIRS) to acquire IR spectra of CO adsorbed on a β -Mo₂C foil at 104 K (29). The position of this band was found to be coverage dependent and shifted from 2054 cm⁻¹ at low CO coverage to 2069 cm⁻¹ at saturation coverage. The authors assigned this ν_{CO} band to a terminally bound CO species and noted that its stretching frequency is characteristic of terminally bonded CO on group VIII metals such as ruthenium. Finally, if the β -Mo₂C foil was exposed to O₂ prior to dosing with CO, the ν_{CO} band broadened and became asymmetric with what appears to be a shoulder at \sim 2125 cm⁻¹.

Additional information concerning the assignment of ν_{CO} bands in the IR spectrum of CO on an activated Mo₂C/Al₂O₃ catalyst can also be gleaned from transmission IR studies of adsorbed CO on mildly reduced and sulfided Mo/Al₂O₃ catalysts. DeCanio and Storm investigated the adsorption of CO on mildly reduced Mo/Al₂O₃ catalysts with a range of Mo loadings (30). Infrared band positions in the ν_{CO} region were found to be dependent upon both the CO coverage and how recently the catalyst had been calcined prior to insertion into the IR cell. A 12 wt% Mo/Al₂O₃ catalyst reduced at 703 K and then exposed to an equilibrium pressure of 20 Torr of CO at room temperature revealed three absorbance features with band positions at 2175, \sim 2130, and 2050 cm⁻¹. Evacuation of the CO resulted in shifts of the first and last peaks to 2190 and 2070 cm⁻¹, respectively, and the disappearance of the band at 2130 cm⁻¹.

The authors assigned the bands at 2175 and 2050 cm⁻¹ to CO bonded to *cus*Mo⁴⁺ and Mo²⁺ species, respectively, and the band at 2130 cm⁻¹ to physisorbed CO.

In a recent study, Kn zinger and coworkers reported the results of an IR investigation of adsorbed CO on a sulfided 7.2 wt% Mo/Al₂O₃ catalyst (31). Depending on the temperature at which the freshly sulfided catalyst was reduced in flowing H₂, one or two ν_{CO} bands were observed following exposure of the catalyst to CO at 77 K. The most intense band, seen previously in a number of laboratories, is located at 2110 cm⁻¹ and has been assigned to CO adsorbed on *cus* Mo²⁺ species located on edge planes of MoS₂ crystallites. A second, weaker band located at 2060 cm⁻¹ is sensitive to the temperature at which the freshly sulfided catalyst is reduced and is assigned to CO bonded to *cus* Mo²⁺ sites located on the corners of MoS₂ crystallites. Considering the results of the three studies described above, the following assignments can tentatively be made for the IR spectrum of CO on an activated 20 wt% Mo₂C/Al₂O₃ catalyst (Fig. 1). The peak at 2178 cm⁻¹ is assigned to CO bonded to *cus* Mo⁴⁺ sites; it should be noted this absorbance feature is actually composed of at least two peaks, the first associated with CO on *cus* Mo⁴⁺ sites ($\nu_{\text{CO}} = \sim$ 2178 cm⁻¹) and a second, much smaller one associated with CO on *cus* Al³⁺ sites ($\nu_{\text{CO}} = 2199$ cm⁻¹) of the uncovered alumina support. The absorbance feature at 2060 cm⁻¹ is assigned to CO adsorbed on *cus* Mo²⁺ species.

TPD of CO on Passivated and Activated 20 wt% Mo₂C/Al₂O₃ Catalysts

As mentioned above, CO TPD experiments were carried out following acquisition of IR spectra for a passivated and activated 20 wt% Mo₂C/Al₂O₃ catalyst; the TPD spectra are shown in Fig. 2. Consistent with our IR spectroscopy assignment, CO TPD from a passivated catalyst produces a single desorption feature with maximum rate of desorption at 190 K which is close to the temperature range 170–185 K at which CO desorbs from pure γ -Al₂O₃ (23). The CO TPD spectrum from the activated 20 wt% Mo₂C/Al₂O₃ catalyst exhibits two desorption features, a peak with maximum rate of desorption at 210 K and a shoulder at \sim 350 K. This spectrum can be compared to CO TPD spectra for four related systems: a carbon modified Mo(100) single crystal (32), a Mo(110) single crystal with a surface carbide layer (28), a molybdenum carbide foil (29), and a 5 wt% Mo₂C/Al₂O₃ catalyst (14). The TPD spectra for the first three systems were acquired under UHV conditions similar to those used in this study, while the TPD spectrum for the 5 wt% Mo₂C/Al₂O₃ catalyst was acquired for CO desorbing into a flow of He. For a Mo(100) single crystal with a monolayer coverage of carbidic carbon, the CO TPD spectrum consists of a single peak with a maximum rate of desorption at \sim 325 K (32). Fr berger and Chen

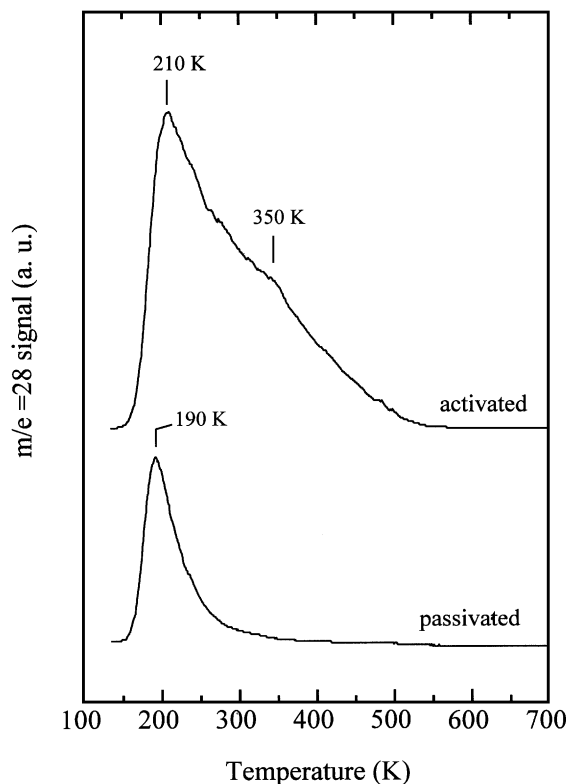


FIG. 2. TPD spectra for CO on a passivated and activated 20% $\text{Mo}_2\text{C}/\text{Al}_2\text{O}_3$ catalyst. The TPD spectra were acquired in UHV following acquisition of the IR spectra shown in Fig. 1.

observed a large desorption peak at 336 K and a smaller, second peak at 1023 K for CO desorbing from a Mo(110) single crystal with a surface carbide layer (28). The former peak is assigned to molecularly bonded CO, while the latter peak is assigned to recombinative desorption of dissociated CO. The CO TPD spectrum obtained by Wang *et al.* for a β - Mo_2C foil displays three CO desorption features—at 155, 325, and 1200 K—one of which, the high temperature peak, is assigned to recombinative desorption of CO (29). The authors believe the low temperature peak may be due to CO desorbing from the sample holder, while the peak at 325 K is assigned to desorption of molecularly bonded CO. Finally, Lee and coworkers observed CO TPD peaks at ~ 250 and ~ 400 K for a 5 wt% $\text{Mo}_2\text{C}/\text{Al}_2\text{O}_3$ catalyst, both of which are assigned to molecularly adsorbed CO species (14). The CO TPD spectrum obtained in this study for an activated 20 wt% $\text{Mo}_2\text{C}/\text{Al}_2\text{O}_3$ catalyst is in general agreement with the results of these related studies. In each case, a desorption feature is observed at or slightly above room temperature (325–400 K). While this range is admittedly broad, comparing desorption maxima is complicated because of the different morphologies of the carbide materials (i.e., bulk vs supported) and the different TPD conditions.

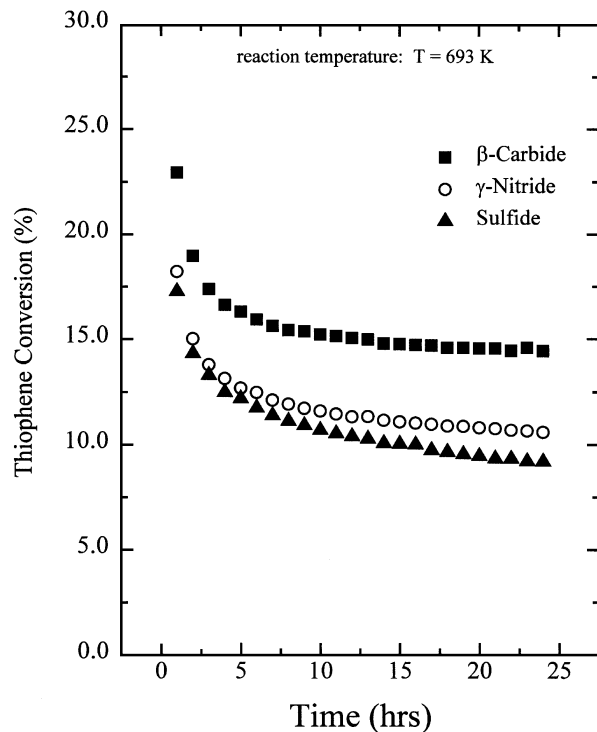


FIG. 3. Thiophene conversion as a function of time for HDS over alumina-supported molybdenum carbide, molybdenum nitride, and sulfided Mo catalysts with 10 wt% Mo loadings.

HDS Catalytic Properties of $\text{Mo}_2\text{C}/\text{Al}_2\text{O}_3$ and $\text{Mo}_2\text{N}/\text{Al}_2\text{O}_3$ Catalysts

Thiophene conversion data at 693 K for alumina-supported Mo carbide, nitride, and sulfided Mo catalysts, all with 10 wt% Mo loading, are shown in Fig. 3. Steady state HDS activity was achieved after ~ 18 h for the $\text{Mo}_2\text{C}/\text{Al}_2\text{O}_3$ catalyst, while the activities of the $\text{Mo}_2\text{N}/\text{Al}_2\text{O}_3$ and sulfided $\text{Mo}/\text{Al}_2\text{O}_3$ catalysts continued to decrease slowly after 24 h on stream. The thiophene HDS activities for the three catalysts after 24 h at 693 K are listed in Table 2. The activities reported have been normalized per mole of molybdenum and are average values for at least three measurements using catalysts prepared in different batches. The product distributions for the catalysts are given in Fig. 4. The only

TABLE 2
Thiophene HDS Activities for Catalysts
with 10 wt% Mo Loading

Catalyst	HDS activity ^a ($\mu\text{mol Th}/\text{mol Mo}/\text{s}$)	Relative HDS activity
Sulfided $\text{Mo}/\text{Al}_2\text{O}_3$	591	1.00
$\text{Mo}_2\text{N}/\text{Al}_2\text{O}_3$	646	1.09
$\text{Mo}_2\text{C}/\text{Al}_2\text{O}_3$	891	1.51

^a Measured after 24 h at 693 K.

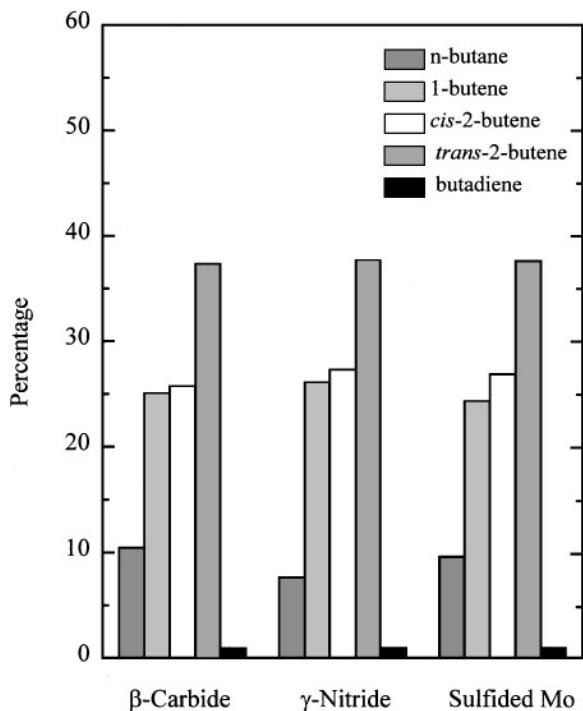


FIG. 4. Product distributions for thiophene HDS over alumina-supported molybdenum carbide, molybdenum nitride, and sulfided Mo catalysts with 10 wt% Mo loadings.

hydrocarbon products detected other than those shown in Fig. 4 were C_1 – C_3 hydrocarbons, which amounted to well under than 1% of the total products. As suggested by the data presented in Fig. 4, the product distributions do not differ significantly for the alumina-supported Mo carbide, nitride, and sulfided Mo catalysts.

The thiophene HDS product distributions and relative activities measured in this study are consistent with those reported by others. While not giving the percentages of the different products, Lee and Boudart reported that bulk α - $MoC_{(1-x)}$ ($x=0.5$) and a sulfided Mo/Al_2O_3 catalyst had indistinguishable thiophene HDS product distributions (11). For nitride catalysts, the product distribution determined here for a 10 wt% Mo_2N/Al_2O_3 catalyst is similar to that obtained by Markel and Van Zee for a bulk Mo_2N catalyst (12). As noted by these authors, the product distribution for thiophene HDS over bulk molybdenum nitride yields butene isomer ratios similar to those predicted for thermodynamic equilibrium of the isomers: *cis*-2 butene/*trans*-2-butene = 0.70, 1-butene/2-butene = 0.34 (31). Using the product distribution data for the 10 wt% Mo_2N/Al_2O_3 catalyst (Fig. 4), such calculations yield ratios quite close to those predicted thermodynamically: *cis*-2-butene/*trans*-2-butene = 0.72, 1-butene/2-butene = 0.40.

The relative HDS activities reported in Table 2 can be compared to those obtained by others. Nagai and coworkers found alumina-supported Mo_2N to be 1.1–1.2 times more

active than an alumina-supported sulfided Mo catalyst for dibenzothiophene HDS (13). Normalizing their activities using surface areas, Markel and Van Zee found bulk Mo_2N to be as active as or more active than bulk MoS_2 depending on the surface area of the nitride (12).

X-Ray Diffraction Analysis of 30 wt% Mo_2C/Al_2O_3 and Mo_2N/Al_2O_3 Catalysts before and after Thiophene HDS

X-ray diffraction patterns were acquired for 30 wt% Mo_2C/Al_2O_3 and Mo_2N/Al_2O_3 catalysts before and after 24 h on stream in a flow reactor. The reactor conditions were identical to those used for the kinetic studies ($T=693$ K); tested catalysts were passivated prior to transfer to an X-ray diffractometer. X-ray diffraction patterns for the fresh and tested catalysts along with those for the alumina support and the bulk Mo phase are shown for carbide and nitride catalysts in Figs. 5 and 6, respectively. The X-ray diffraction patterns for the 30 wt% Mo_2C/Al_2O_3 and Mo_2N/Al_2O_3 catalysts following 24 h on stream in the flow reactor at 693 K are essentially unchanged from those of the fresh catalysts, indicating that the alumina-supported β - Mo_2C and γ - Mo_2N crystallites are resistant to bulk sulfidation under thiophene

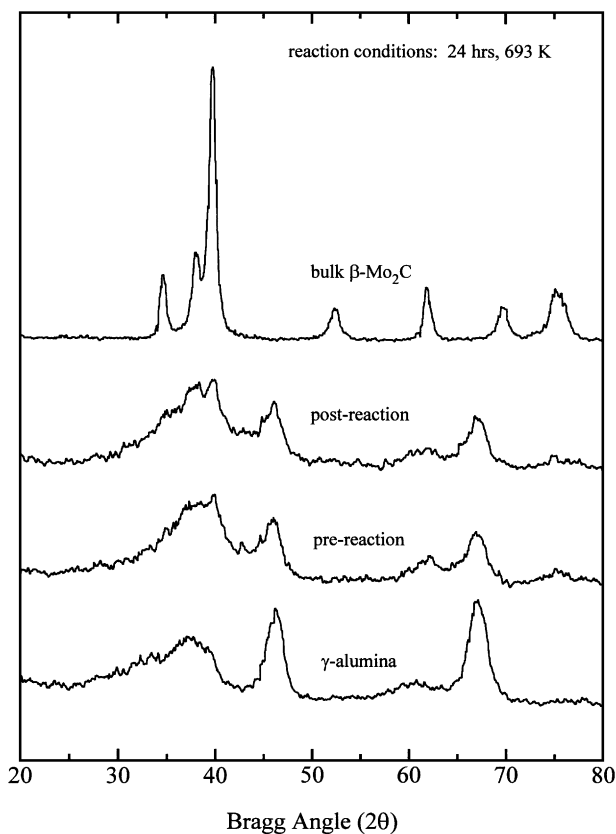


FIG. 5. X-ray diffraction patterns for γ - Al_2O_3 and bulk β - Mo_2C as well as a 30 wt% Mo_2C/Al_2O_3 catalyst before and after 24 h on stream in the thiophene HDS flow reactor at 693 K.

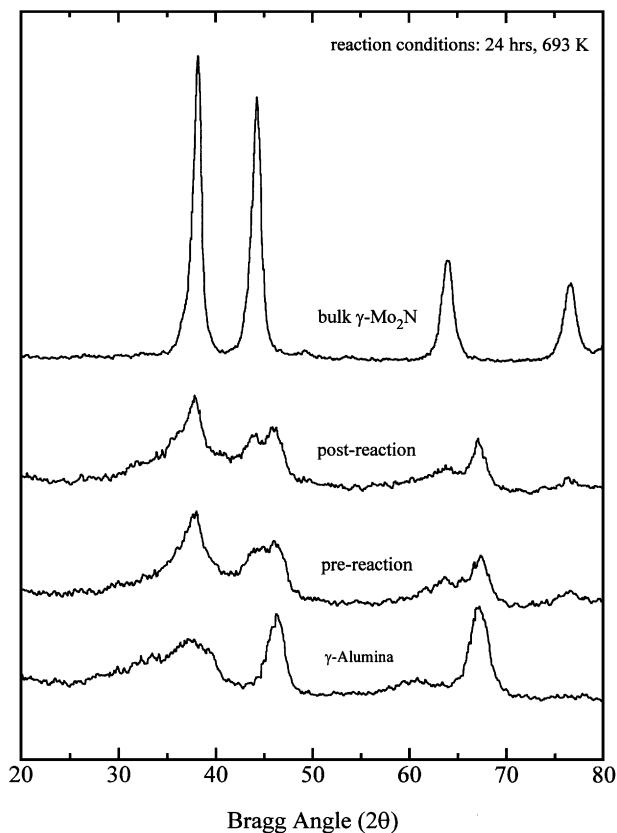


FIG. 6. X-ray diffraction patterns for γ - Al_2O_3 and bulk γ - Mo_2N as well as a 30 wt% $\text{Mo}_2\text{N}/\text{Al}_2\text{O}_3$ catalyst before and after 24 h on stream in the thiophene HDS flow reactor at 693 K.

HDS conditions. Markel and Van Zee obtained similar results for bulk γ - Mo_2N catalysts used on stream in a thiophene HDS reactor at 673 K or subjected to sulfidation in a 10% $\text{H}_2\text{S}/\text{H}_2$ mixture at temperatures as high as 823 K (12). For thiophene HDS carried out at 573 K, Lee and Boudart observed the structure of bulk α - $\text{MoC}_{(1-x)}$ ($x=0.5$) to be retained following 8 h on stream (11). To our knowledge, the results presented here are the first which indicate that supported β - Mo_2C and γ - Mo_2N crystallites, estimated to have particle sizes of ~ 60 Å for the catalysts investigated, retain their bulk structure when subjected to the sulfiding conditions found in a thiophene HDS reactor.

IR Spectroscopy of Adsorbed CO on 10 wt% $\text{Mo}_2\text{C}/\text{Al}_2\text{O}_3$, $\text{Mo}_2\text{N}/\text{Al}_2\text{O}_3$ and Sulfided $\text{Mo}/\text{Al}_2\text{O}_3$ Catalysts Treated in a Thiophene/ H_2 Mixture

In order to further investigate the effect of sulfiding conditions on the alumina-supported carbide and nitride catalysts, IR spectroscopy was used to probe changes in adsorption sites on 10 wt% $\text{Mo}_2\text{C}/\text{Al}_2\text{O}_3$ and $\text{Mo}_2\text{N}/\text{Al}_2\text{O}_3$ catalysts treated in static thiophene/ H_2 mixtures. Following exposure of a catalyst sample to a thiophene/ H_2 mixture at elevated temperatures, the sample was evacuated to UHV

pressures, outgassed at 750 K and then exposed to 5.0 Torr of CO at 298 K prior to acquiring the IR spectra. For comparison purposes, this same set of treatments was carried out for a 10 wt% sulfided $\text{Mo}/\text{Al}_2\text{O}_3$ catalyst as displayed in Fig. 7. The IR spectra of adsorbed CO on the sulfided catalyst treated in thiophene/ H_2 mixtures at temperatures in the range 400–700 K are essentially unchanged from that of the freshly sulfided catalyst. As discussed earlier, the single ν_{CO} band at 2105 cm^{-1} is characteristic of CO adsorbed on sulfided $\text{Mo}/\text{Al}_2\text{O}_3$ catalysts and has been assigned by others to CO bonded to *cus* Mo^{2+} sites (20). Shown in Figs. 8 and 9 are IR spectra in the ν_{CO} region for 10 wt% Mo carbide and nitride catalysts which have been freshly activated or heated to the given temperatures in thiophene/ H_2 mixtures. Focussing initially on the IR spectra for the freshly activated catalysts, the ν_{CO} features for adsorbed CO are quite similar for the 10 wt% Mo nitride and carbide catalysts and also with those for a 20 wt% $\text{Mo}_2\text{C}/\text{Al}_2\text{O}_3$ catalyst; the IR spectrum in the ν_{CO} region for this last catalyst was described in detail earlier (Fig. 1). In contrast to what was observed for the sulfided Mo catalyst, significant changes are observed for the carbide and nitride catalysts when heated in the thiophene/ H_2 mixture at temperatures in the range 400–700 K. A gradual transformation of the IR spectrum occurs in both cases from that of CO adsorbed on freshly

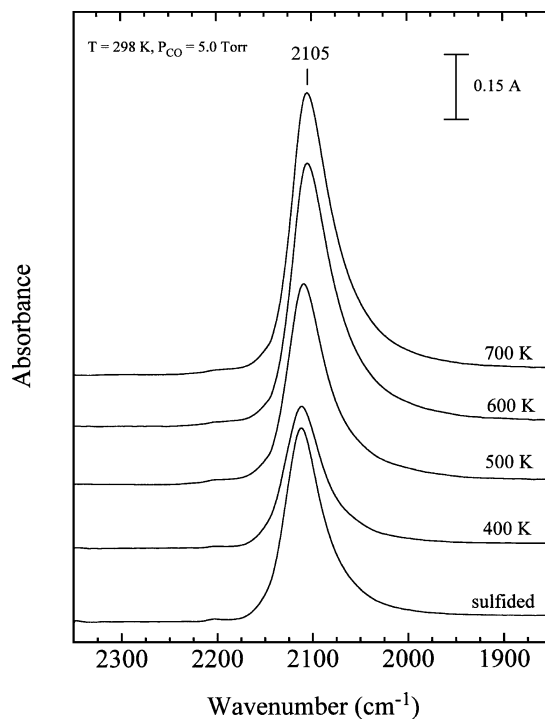


FIG. 7. IR spectra in the ν_{CO} region for a freshly sulfided 10 wt% $\text{Mo}/\text{Al}_2\text{O}_3$ catalyst and the same catalyst treated in a thiophene/ H_2 mixture ($P_{\text{Th}} = 5.0$ Torr, $P_{\text{H}_2} = 755$ Torr) at the given temperatures for 1 h. Following the thiophene/ H_2 treatments, the catalyst was outgassed in UHV at 750 K prior to CO adsorption at 298 K.

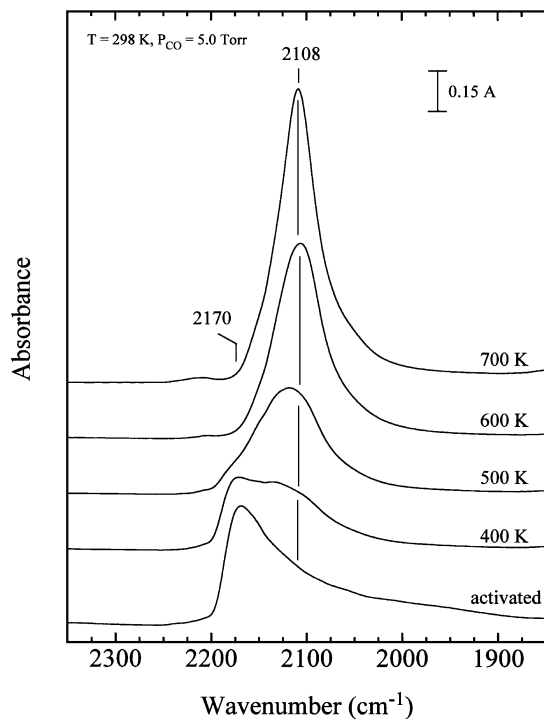


FIG. 8. IR spectra in the ν_{CO} region for a freshly activated 10 wt% $\text{Mo}_2\text{C}/\text{Al}_2\text{O}_3$ catalyst and the same catalyst treated in a thiophene/ H_2 mixture ($P_{\text{Th}} = 5.0$ Torr, $P_{\text{H}_2} = 755$ Torr) at the given temperatures for 1 h. Following the thiophene/ H_2 treatments, the catalyst was outgassed in UHV at 750 K prior to CO adsorption at 298 K.

activated carbide and nitride catalysts to one resembling CO adsorbed on a sulfide catalyst for treatment temperatures of 600 K and above. Noting that HDS is typically carried out at temperatures near 600 K or higher, it is likely that the surfaces of alumina-supported Mo carbide and nitride catalysts under reaction conditions resemble those of sulfided Mo catalysts.

Chemisorption Capacities of Sulfided 10 wt% $\text{Mo}_2\text{C}/\text{Al}_2\text{O}_3$ and $\text{Mo}_2\text{N}/\text{Al}_2\text{O}_3$ Catalysts

Given that the results described above indicate that the surface of carbide and nitride catalysts become sulfided un-

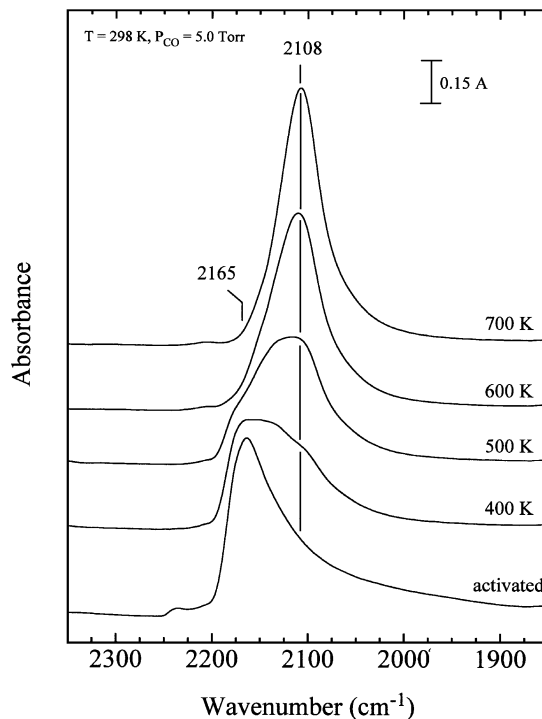


FIG. 9. IR spectra in the ν_{CO} region for a freshly activated 10 wt% $\text{Mo}_2\text{N}/\text{Al}_2\text{O}_3$ catalyst and the same catalyst treated in a thiophene/ H_2 mixture ($P_{\text{Th}} = 5.0$ Torr, $P_{\text{H}_2} = 755$ Torr) at the given temperatures for 1 h. Following the thiophene/ H_2 treatments, the catalyst was outgassed in UHV at 750 K prior to CO adsorption at 298 K.

der HDS conditions, CO and/or O_2 chemisorption measurements of freshly activated catalysts may not be the best method for estimating the number of active catalytic sites. To this end, CO and O_2 chemisorption measurements were carried out for 10 wt% $\text{Mo}_2\text{C}/\text{Al}_2\text{O}_3$ and $\text{Mo}_2\text{N}/\text{Al}_2\text{O}_3$ catalysts, which were sulfided using conditions identical to those for preparation of a 10 wt% sulfided Mo/ Al_2O_3 catalyst. For comparison purposes, Table 3 lists the CO and O_2 chemisorption capacities of freshly activated carbide and nitride catalysts along side those for the sulfided catalysts. In the case of the sulfided Mo catalyst, the only value listed is for the freshly sulfided catalyst. Sulfidation of the carbide and nitride catalysts results in a substantial decrease in both their CO and O_2 chemisorption capacities. If it is assumed that the HDS activities of alumina-supported Mo carbide and nitride catalysts correlate with their sulfided state CO and O_2 chemisorption capacities, thiophene HDS turnover frequencies can be calculated as listed in Table 4.

DISCUSSION

The major results of this study can be summarized as follows: (1) CO adsorption on freshly activated $\text{Mo}_2\text{C}/\text{Al}_2\text{O}_3$ catalysts occurs on *cus* Mo^{4+} and Mo^{2+} sites, (2) the thiophene HDS activities of alumina-supported Mo sulfide,

TABLE 3

Effect of Sulfidation on Chemisorption Capacities for Catalysts with 10 wt% Mo Loading

Catalyst	CO uptake (273 K) ($\mu\text{mol CO/g}$)		O_2 uptake (196 K) ($\mu\text{mol O}_2/\text{g}$)	
	Freshly reduced	Freshly sulfided	Freshly reduced	Freshly sulfided
Sulfided Mo/ Al_2O_3	—	37	—	50
$\text{Mo}_2\text{N}/\text{Al}_2\text{O}_3$	78	49	115	59
$\text{Mo}_2\text{C}/\text{Al}_2\text{O}_3$	69	53	111	57

TABLE 4

Thiophene HDS Turnover Frequencies After 24 h at 693 K

Catalyst	Turnover frequency	
	Based upon titration of sites with CO	Based upon titration of sites with O ₂
Sulfided Mo/Al ₂ O ₃	0.0159 s ⁻¹	0.0117 s ⁻¹
Mo ₂ N/Al ₂ O ₃	0.0136	0.0114
Mo ₂ C/Al ₂ O ₃	0.0174	0.0161

nitride and carbide catalysts, normalized per mole of molybdenum, increase according to the trend sulfided Mo < γ -Mo₂N < β -Mo₂C, and (3) the surfaces of alumina-supported β -Mo₂C and γ -Mo₂N particles become sulfided under thiophene HDS conditions while their bulk structure is retained. To our knowledge, this is the first study to appear in the literature which directly compares the HDS activities of alumina-supported Mo carbide, nitride, and sulfided Mo catalysts and investigates the effect of sulfiding conditions on their bulk structure and adsorption properties.

As mentioned in the Introduction, early transition metal carbides and nitrides have drawn considerable interest in the catalysis community because of similarities between their catalytic properties and those of a number of group VIII metals (2). An understanding of the modification of the catalytic properties of early transition metals by the formation of interstitial alloys with the nonmetallic elements carbon and nitrogen is not well understood. In their seminal investigation of the catalytic properties of tungsten carbide, Levy and Boudart suggested that the platinum-like catalytic properties of tungsten carbide are due to the donation of valence electrons from carbon to tungsten (34). Oyama has examined trends in melting point, stoichiometry, and crystal structures and concluded that the formation of Mo and W carbides and nitrides results in greater electron occupancy of the *spd* bands of the metals, rendering them more noble metal-like in their catalytic properties (35). More recently, near edge X-ray absorption fine structure (NEXAFS) has been used by Chen to examine a surface carbide layer on a Mo(110) single crystal (36). The NEXAFS experiments yielded an estimation of Mo^{0.2±0.2} for the oxidation state of Mo in the carbide layer, indicating that the bonding between Mo and carbon is largely covalent in nature.

The IR spectroscopy results presented here for an activated 20 wt% Mo₂C/Al₂O₃ catalyst (Fig. 1) indicate that CO adsorbs on *cus* Mo⁴⁺ and Mo²⁺ ions exposed on the catalyst surface. Given the NEXAFS results described above along with those of the HREELS and RAIRS studies discussed in the Results section, it is likely that a significant amount of oxygen has been incorporated into the alumina-supported β -Mo₂C particles and cannot be removed by

heating to 750 K in flowing H₂. The IR spectrum shown in Fig. 9 for CO adsorbed on a freshly activated 10 wt% Mo₂N/Al₂O₃ catalyst indicates that this is also true for alumina-supported γ -Mo₂N. A recent study by Sajkowski and Oyama also suggests that alumina-supported β -Mo₂C contains a significant amount of oxygen (5). X-ray photoelectron spectroscopy (XPS) analysis of Mo₂C/Al₂O₃ catalysts reduced at 693 K in flowing H₂ indicated that molybdenum was present in oxidation states of Mo⁴⁺ and higher. Additional evidence for oxygen incorporation into the supported Mo carbide and nitride particles comes from the study of Wang *et al.* of CO adsorption on a β -Mo₂C foil (29). IR spectra were acquired for adsorbed CO on a β -Mo₂C foil both by itself and in the presence of preadsorbed oxygen. Adsorbed CO on the clean β -Mo₂C foil gave rise to a ν_{CO} band at 2069 cm⁻¹; exposure of the carbide foil to O₂ prior to dosing with CO resulted in growth of a shoulder at ~2125 cm⁻¹. This shoulder is presumably associated with CO adsorbed on an oxidized Mo site. For the 10 wt% Mo₂C/Al₂O₃ catalyst investigated here a ν_{CO} band is observed at 2178 cm⁻¹ with a shoulder at 2060 cm⁻¹, with the former suggesting the presence of oxidized Mo sites on the surface of the catalyst.

Further insight into the CO adsorption sites on freshly activated Mo₂C/Al₂O₃ carbide catalysts is revealed in the TPD spectra from this and related studies. The CO TPD spectrum for an activated 20 wt% Mo₂C/Al₂O₃ catalyst (Fig. 2) exhibits two desorption features, a peak with maximum rate of desorption at 210 K and a shoulder at ~350 K. As discussed in the Results section, a high temperature desorption feature is also observed for CO TPD from a number of related materials with the important difference that it is the largest desorption feature in these spectra. For a β -Mo₂C foil (29) and a carbided Mo(110) single crystal (28), this desorption feature is located at 325 and 336 K, respectively. In the case of the β -Mo₂C foil this peak is associated with a ν_{CO} band at 2069 cm⁻¹, while for the carbided Mo(110) single crystal it is associated with both bridge ($\nu_{\text{CO}} = 1850$ cm⁻¹) and terminal ($\nu_{\text{CO}} = 2015$ cm⁻¹) bonded CO species. It is likely, then, that the high temperature shoulder in the CO TPD spectrum acquired here for a 20 wt% Mo₂C/Al₂O₃ catalyst is associated with the ν_{CO} band at 2060 cm⁻¹. This conclusion is supported by the results of experiments not reported here in which IR spectra acquired during TPD show the preferential decrease in the intensity of the ν_{CO} band at 2178 cm⁻¹ at low temperatures followed by the decrease in intensity of the 2060 cm⁻¹ feature at higher temperatures. As described in the Results section, ν_{CO} bands in the 2050–2060 cm⁻¹ range have been assigned to CO adsorbed on *cus* Mo²⁺ sites of mildly reduced and sulfided Mo/Al₂O₃ catalysts (30, 31).

Focussing on supported Mo carbide catalysts, Lee and co-workers have utilized CO TPD (in a He flow) to characterize adsorption sites on 5 wt% Mo₂C/Al₂O₃ catalysts and

have also observed two desorption features, albeit at the higher temperatures of ~ 250 and ~ 400 K (14). Interestingly, the relative intensities of the two desorption features are approximately the reverse of those observed in this study for a 20 wt% $\text{Mo}_2\text{C}/\text{Al}_2\text{O}_3$ catalyst. There are at least two possible explanations for these different observations. The first concerns the difference in Mo loading but experiments performed in our laboratory for carbide catalysts with Mo loadings in the range 5–20 wt% Mo showed no significant change in the relative intensities of the two desorption features (37). The second explanation focuses on pretreatment of the catalysts prior to CO exposure and acquisition of the TPD spectrum. In their study, Lee and coworkers synthesized the 5 wt% $\text{Mo}_2\text{C}/\text{Al}_2\text{O}_3$ catalyst *in situ* and therefore were able to acquire the CO TPD spectrum without intervening passivation and activation. Experiments carried out in our laboratory indicate that the CO chemisorption capacity of $\text{Mo}_2\text{C}/\text{Al}_2\text{O}_3$ catalysts submitted to the passivation/activation procedure described in the Experimental section is approximately half that of freshly synthesized carbide catalysts with the same Mo loading (38). This suggests oxygen adsorbed onto the catalyst surface during passivation cannot be completely removed by activation in flowing H_2 . Returning now to the CO TPD spectrum for the activated 20 wt% $\text{Mo}_2\text{C}/\text{Al}_2\text{O}_3$ catalyst, it is likely that the desorption feature at 210 K is associated with more oxidized Mo sites (e.g. Mo^{4+}) while the feature at ~ 350 K is associated with sites characteristic of molybdenum carbide, and tentatively assigned here to Mo^{2+} species based upon the IR data discussed above.

The thiophene HDS activities ($\mu\text{mol Th/mol Mo/s}$) measured in this study (Table 2) clearly indicate that alumina-supported $\beta\text{-Mo}_2\text{C}$ and $\gamma\text{-Mo}_2\text{N}$ are more active HDS catalysts than a sulfided $\text{Mo}/\text{Al}_2\text{O}_3$ catalyst with the same Mo loading. These results provide further evidence that early transition metal carbides and nitrides display strong potential for use in the commercial HDS process. To improve our knowledge of the HDS catalytic properties of these materials, one of the focuses of this study was to gain a better understanding of the nature of the active catalyst. To this end, the bulk structure and surfaces of carbide and nitride catalysts were investigated before and after use in a thiophene HDS reactor or treatment in conditions mimicking those of the reactor. Consistent with the results of others for bulk $\gamma\text{-Mo}_2\text{N}$ (12) and $\alpha\text{-MoC}_{(1-x)}$ ($x \approx 0.5$) catalysts (11), the crystalline structure of the Mo containing phase in 30 wt% $\text{Mo}_2\text{C}/\text{Al}_2\text{O}_3$ and $\text{Mo}_2\text{N}/\text{Al}_2\text{O}_3$ catalysts was found to be retained following 24 h on stream in a catalytic reactor (Figs. 5 and 6).

While X-ray diffraction indicates that the bulk structure of alumina-supported $\beta\text{-Mo}_2\text{C}$ and $\gamma\text{-Mo}_2\text{N}$ particles is preserved under HDS reaction conditions, the surface of supported carbide and nitride particles becomes sulfided when heated in the presence of a thiophene/ H_2 mixture. Using

IR spectroscopy to monitor the stretching frequency of adsorbed CO, it was possible to observe the conversion of adsorption sites on the surface of supported carbide and nitride particles to sites essentially identical to those on a sulfided $\text{Mo}/\text{Al}_2\text{O}_3$ catalyst (Figs. 7–9). This transformation begins as a result of heating 10 wt% $\text{Mo}_2\text{C}/\text{Al}_2\text{O}_3$ and $\text{Mo}_2\text{N}/\text{Al}_2\text{O}_3$ catalysts in a thiophene/ H_2 mixture at temperatures as low as 400 K and adsorption sites on the carbide and nitride catalysts are essentially indistinguishable from those on a sulfide catalyst following such a treatment at 600 K. Unfortunately, the X-ray diffraction and IR spectroscopy studies could not be done on catalysts with the same weight loading and, as a result, it can only be inferred that sulfidation is limited to the exterior of the supported 10 wt% Mo carbide and nitride particles, as depicted in Fig. 10. Using X-ray photoelectron spectroscopy (XPS), Sajkowski and Oyama observed some sulfur incorporation into the surface region of a $\text{Mo}_2\text{C}/\text{Al}_2\text{O}_3$ catalyst used for HDN and HDS of a coal derived feed containing both sulfur and nitrogen impurities (5). While the concentration of sulfur compounds in the feed was low ($<0.1\%$), the authors could not rule out the possibility of MoS_2 formation on the topmost atomic layers of the carbide particles.

As discussed in the Introduction, an important concern when comparing the catalytic activities of different catalysts is the means by which the active sites are estimated. For sulfided Mo catalysts, O_2 chemisorption has traditionally been employed to titrate active sites while CO chemisorption has been utilized for carbide and nitride catalysts. Hydrodesulfurization activity has been shown to correlate with the chemisorption capacity of Mo sulfide catalysts for both of these probe molecules (15–17). Given that the results of this study indicate that the surfaces of alumina-supported $\beta\text{-Mo}_2\text{C}$ and $\gamma\text{-Mo}_2\text{N}$ particles become sulfided under HDS reaction conditions, one might expect that either the CO or O_2 chemisorption capacities of *sulfided* $\text{Mo}_2\text{C}/\text{Al}_2\text{O}_3$ and $\text{Mo}_2\text{N}/\text{Al}_2\text{O}_3$ catalysts would be a suitable measure of the number of active HDS sites for these catalysts. To this end, CO and O_2 chemisorption capacities were measured for 10 wt% $\text{Mo}_2\text{C}/\text{Al}_2\text{O}_3$ and $\text{Mo}_2\text{N}/\text{Al}_2\text{O}_3$ catalysts which were sulfided under conditions identical

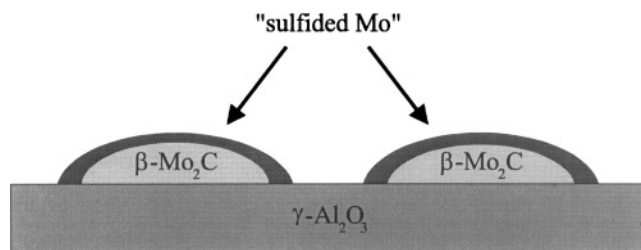


FIG. 10. Schematic representation of a $\text{Mo}_2\text{C}/\text{Al}_2\text{O}_3$ catalyst during thiophene HDS. A similar structure is proposed for $\text{Mo}_2\text{N}/\text{Al}_2\text{O}_3$ catalysts under reaction conditions.

to those used to prepare sulfided Mo/Al₂O₃ catalysts (see Experimental section). The CO and O₂ chemisorption capacities of the freshly sulfided and, for comparison purposes, reduced catalysts are listed in Table 3. The CO and O₂ chemisorption capacities of the freshly sulfided catalysts differ significantly from those of the freshly reduced catalysts. For alumina-supported Mo carbide and nitride catalysts used in the sulfiding conditions present in a HDS reactor, it is likely that the CO and O₂ chemisorption capacities of the freshly sulfided catalysts provide a more accurate estimate of the number of active sites than do those of the freshly reduced catalysts. Listed in Table 4 are thiophene HDS turnover frequencies calculated using the CO and O₂ chemisorption capacities of freshly sulfided 10 wt% Mo carbide, nitride, and sulfide catalysts as a measure of the active sites for the three catalysts. These turnover frequencies can be compared to those determined in two related studies. Using room temperature CO and O₂ chemisorption to quantify active sites for Mo₂C/Al₂O₃ and sulfided Mo/Al₂O₃ catalysts, respectively, Sajkowski and Oyama observed the supported Mo carbide catalyst to be three times more active than the sulfided Mo catalyst for HDS of a coal-derived liquid feed (4, 5). Only relative turnover frequencies were reported in this study. Lee and Boudart reported an initial thiophene HDS turnover frequency of slightly less than $1.0 \times 10^{-3} \text{ s}^{-1}$ for unsupported α -MoC_(1-x) ($x = 0.5$) at a reaction temperature of 573 K (11). These authors also estimated the number of active sites on the unsupported carbide catalyst via room temperature CO chemisorption.

IR spectroscopy of adsorbed CO on 10 wt% Mo₂C/Al₂O₃ and Mo₂N/Al₂O₃ catalysts treated in thiophene/H₂ mixtures at temperatures of 600 K and above indicates that the adsorption sites on these catalysts are essentially identical to those exposed on a sulfided 10 wt% Mo/Al₂O₃ catalyst. The similarity in CO adsorption properties of the sites on the three catalysts suggests not only that the surfaces of the carbide and nitride catalysts become sulfided, but also that the catalysts should exhibit similar thiophene HDS activities on a per site basis. Reference to the thiophene HDS turnover frequencies listed Table 4 shows that while they are not identical, they are somewhat more closely grouped than the HDS activities reported in Table 2, which were calculated based upon their Mo content. In keeping with the model for the active catalytic surface presented in Fig. 10, it is tempting to conclude that the β -Mo₂C and γ -Mo₂N particles act as supports on which a thin layer of sulfided Mo forms under HDS conditions. Combining the properties of high melting point, hardness, and strength (2), the molybdenum carbide and nitride particles may serve as rigid substrates for a sulfided Mo phase exposing large numbers of *cus* Mo sites on which thiophene adsorption and reaction could occur. Indeed, recent IR spectroscopy results reported by Knözinger and coworkers suggest that

morphological changes occur in sulfided Mo slabs present on the surface of a sulfided Mo/Al₂O₃ catalyst treated in flowing hydrogen at temperatures in the range 453–773 K (31). Mo²⁺ sites thought to exist at the corners of sulfided Mo slabs ($\nu_{\text{CO}} = 2060 \text{ cm}^{-1}$) disappear upon being heated in flowing H₂ at 773 K. The authors suggest that slab growth may occur under these conditions, leading to a decrease in the ratio of corner to edge sites. In the case of the Mo₂C/Al₂O₃ and Mo₂N/Al₂O₃ catalysts, the rigidity of the β -Mo₂C and γ -Mo₂N particles may hinder the mobility of the sulfided Mo layer at their surfaces and therefore help to maintain a higher number of exposed *cus* Mo²⁺ sites under reaction conditions. Of course, this model for the active catalytic surface does not explain why alumina-supported β -Mo₂C was observed to have a significantly higher thiophene HDS activity than a similarly supported γ -Mo₂N catalyst. Interestingly, preliminary thiophene HDS activity measurements of alumina-supported α -MoC_(1-x) ($x \approx 0.5$) suggest that it has an activity closer to that of γ -Mo₂N. It is worth noting that both α -MoC_(1-x) ($x \approx 0.5$) and γ -Mo₂N are face-centered cubic materials, while β -Mo₂C has a hexagonal closed packed lattice structure. Further experiments are planned to explore the effect of the carbide and nitride structure on the morphology of the surface of Mo₂C/Al₂O₃ and Mo₂N/Al₂O₃ catalysts in conditions similar to those found in a thiophene HDS reactor.

CONCLUSION

Alumina-supported molybdenum carbide and nitride catalysts have been shown to have higher activity for the HDS of thiophene, normalized per mole of molybdenum, than a conventional sulfided Mo/Al₂O₃ catalyst with the same Mo loading. Infrared spectroscopy of adsorbed CO on the surface of freshly activated Mo₂C/Al₂O₃ catalysts indicates that CO adsorbs on to *cus* Mo⁴⁺ and Mo²⁺ species exposed at the surface of the catalysts. Comparison of the IR as well as TPD data with related studies published in the literature suggests that there is incorporation of oxygen into alumina-supported β -Mo₂C and γ -Mo₂N particles, even after reduction in flowing H₂ at 750 K.

In the sulfiding conditions found in a thiophene HDS reactor, the surfaces of Mo₂C/Al₂O₃ and Mo₂N/Al₂O₃ catalysts become sulfided as determined by IR spectroscopy of adsorbed CO while X-ray diffraction indicates that the bulk structure of the supported Mo carbide and nitride particles is preserved. In the sulfided state, CO adsorption sites at the surface of Mo₂C/Al₂O₃ and Mo₂N/Al₂O₃ catalysts are essentially identical to those on a sulfided Mo/Al₂O₃ catalyst. A tentative model is proposed to explain the higher activity of the supported Mo carbide and nitride catalysts in which a thin layer of highly dispersed sulfided Mo is present on the surfaces of the carbide and nitride particles.

ACKNOWLEDGMENTS

This research was supported by the National Science Foundation under Grant CHE-9400740 and by Cottrell College Science and Partners in Science Awards of Research Corporation. Acknowledgment is also made to the donors of the Petroleum Research Fund, administered by the ACS, and to the Henry Dreyfus Teacher-Scholar Awards Program of the Camille and Henry Dreyfus Foundation for partial support of this research. The authors also acknowledge Dr. J. G. Chen and Professors S. T. Oyama and P. H. McBreen for helpful discussions and providing copies of manuscripts prior to publication.

REFERENCES

1. Chianelli, R. R., Lyons, J. E., and Mills, G. A., *Catal. Today* **22**, 361 (1994).
2. Oyama, S. T., *Catal. Today* **15**, 179 (1992).
3. Schlatter, J. C., Oyama, S. T., Metcalfe, J. E., and Lambert, J. M., *Ind. Eng. Chem. Res.* **27**, 1648 (1988).
4. Sajkowski, D. J., and Oyama, S. T., *ACS Div. Petrol. Prepr.* **35**, 233 (1990).
5. Sajkowski, D. J., and Oyama, S. T., *Appl. Catal. A* **134**, 339 (1996).
6. Nagai, M., and Miyao, T., *Catal. Lett.* **15**, 105 (1992).
7. Lee, K. S., Abe, H., Reimer, J. A., and Bell, A. T., *J. Catal.* **139**, 34 (1993).
8. Choi, J. G., Brenner, J. R., Colling, C. W., Demczyk, B., Dunning, J. L., and Thompson, L. T., *Catal. Today* **15**, 201 (1992).
9. Abe, H., and Bell, A. T., *Catal. Lett.* **18**, 1 (1993).
10. Colling, C. W., and Thompson, L. T., *J. Catal.* **146**, 193 (1994).
11. Lee, J. S., and Boudart, M., *Appl. Catal.* **19**, 207 (1985).
12. Markel, E. J., and Van Zee, J. W., *J. Catal.* **126**, 643 (1990).
13. Nagai, M., Miyao, T., and Tuboi, T., *Catal. Lett.* **18**, 9 (1993).
14. Lee, J. S., Lee, K. H., and Lee, J. Y., *J. Phys. Chem.* **96**, 362 (1992).
15. Tauster, S. J., Pecoraro, T. A., and Chianelli, R. R., *J. Catal.* **63**, 515 (1980).
16. Bachelier, J., Tilliette, M. J., Duchet, J. C., and Cornet, D., *J. Catal.* **76**, 300 (1982).
17. Bachelier, J., Duchet, J. C., and Cornet, D., *Bull. Soc. Chim. Belg.* **90**, 1301 (1981).
18. Delgado, E., Funetes, G. A., Hermann, C., Kunzmann, G., and Knözinger, H., *Bull. Soc. Chim. Belg.* **93**, 743 (1984).
19. Zaki, M. I., Vielhaber, B., and Knözinger, H., *J. Phys. Chem.* **90**, 3176 (1986).
20. Müller, B., van Langeveld, A. D., Moulijn, J. A., and Knözinger, H., *J. Phys. Chem.* **97**, 9028 (1993).
21. Lee, J. S., Yeom, M. H., Park, K. Y., Nam, I. S., Chung, J. S., Kim, Y. G., and Moon, S. H., *J. Catal.* **128**, 126 (1991).
22. Spies, G. H., and Angelici, R. J., *Organometallics* **6**, 1897 (1987).
23. Diaz, A. L., and Bussell, M. E., *J. Phys. Chem.* **97**, 470 (1993).
24. McClune, W. F. (Ed.), JCPDS Powder Diffraction File (Inorganic), 1992.
25. McClune, W. F. (Ed.), JCPDS Powder Diffraction File (Inorganic), 1992.
26. Unpublished results.
27. Ballinger, T. H., and Yates, J. T., Jr., *Langmuir* **7**, 3041 (1991).
28. Früberger, B., and Chen, J. G., *Surf. Sci.* **342**, 38 (1995).
29. Wang, J., Castonguay, M., McBreen, P. H., Ramanathan, S., and Oyama, S. T., in "Transition Metal Carbides and Nitrides" (S. T. Oyama, Ed.), p. 426. Chapman & Hall, New York, 1996.
30. DeCanio, E. C., and Storm, D. A., *J. Catal.* **130**, 653 (1991).
31. Müller, B., van Langeveld, A. D., Moulijn, J. A., and Knözinger, H., *J. Phys. Chem.* **97**, 9028 (1993).
32. Ko, E. I., and Madix, R. J., *Surf. Sci.* **109**, 221 (1981).
33. Benson, S. W., and Base, A. W., *J. Am. Chem. Soc.* **85**, 1385 (1963).
34. Levy, R. B., and Boudart, M., *Science* **181**, 547 (1973).
35. Oyama, S. T., *J. Solid State Chem.* **96**, 442 (1992).
36. Chen, J. G., *Chem. Rev.* **96**, 1477 (1996).
37. Unpublished results.
38. Unpublished results.